Mon. Not. R. Astron. Soc. **000**, 1–?? (2007) Printed 1 February 2008 (MN LATEX style file v2.2)

Transient growth and coupling of vortex and wave modes in self-gravitating gaseous discs

G. R. Mamatsashvili [1⋆] and G. D. Chagelishvili [1]
[1] *E. Kharadze Georgian National Astrophysical Observatory, 2a Kazbegi Ave., Tbilisi 0160, Georgia*

Accepted 2007 July 26. Received 2007 July 18; in original form 2007 January 28

ABSTRACT
Flow nonnormality induced linear transient phenomena in thin self-gravitating astrophysical discs are studied in the shearing sheet approximation. The considered system includes two modes of perturbations: vortex and (spiral density) wave. It is shown that self-gravity considerably alters the vortex mode dynamics – its transient (swing) growth may be several orders of magnitude stronger than in the non-self-gravitating case and 2-3 times larger than the transient growth of the wave mode. Based on this finding, we comment on the role of vortex mode perturbations in a gravitoturbulent state. Also described is the linear coupling of the perturbation modes, caused by the differential character of disc rotation. The coupling is asymmetric – vortex mode perturbations are able to excite wave mode ones, but not vice versa. This asymmetric coupling lends additional significance to the vortex mode as a participant in spiral density waves and shocks manifestations in astrophysical discs.

Key words: accretion, accretion discs – gravitation – hydrodynamics – instabilities – planetary systems: protoplanetary discs

1 INTRODUCTION

The comprehension of the regular spiral structure of galaxies provided a powerful incentive for the investigation of dynamical processes and phenomena in astrophysical discs. Afterwards the study in this direction intensified and somewhat changed (emphases shifted) – in the 70s of the last century a powerful branch of astrophysical disc research was developed along with the X-ray astronomy. The latter revealed a strong energy release in discs – accretion of the disc matter onto its centre – that is ascribed to anomalous viscosity due to some sort of turbulence (Shakura & Sunyaev 1973; Pringle 1981). In self-gravitating discs, turbulence and angular momentum transport process are commonly attributed to spiral density (SD) waves (Gammie 2001; Lodato & Rice 2004; Lodato & Rice 2005; Mejia et al. 2005). In other words, in the study of self-gravitating discs, attention is focused on the dynamical activity (possibility of amplification) of SD wave perturbations. On the other hand, in investigating turbulence and angular momentum transport in non-self-gravitating discs, the main emphasis is put on the dynamical activity of vortical perturbations (Lominadze, Chagelishvili & Chanishvili 1988; Godon & Livio 1999; Lovelace et al. 1999; Davis, Sheehan & Cuzzi 2000; Ioannou & Kakouris 2001; Tagger 2001; Davis 2002; Chagelishvili et al. 2003; Klahr & Bodenheimer 2003; Tevzadze et al. 2003; Umurhan & Regev 2004; Yecko 2004; Afshordi, Mukhopadhyay & Narayan 2005; Bodo et al. 2005; Johnson & Gammie 2005). Interest to this type of perturbations is also connected with the idea that long-lived vortices in protoplanetary discs play an important role in the planet formation (Barge & Sommeria 1995; Bracco et al. 1999; Godon & Livio 1999; Godon & Livio 2000; Klahr & Bodenheimer 2006). Regular vortex structures are also observed in several spiral galaxies (Fridman & Khoruzhii 1999).

In general, one can say that the astrophysical disc community has been advancing along a crooked path solving dynamical problems. Matters are complicated by one of the main sources supplying energetically dynamical processes in discs – differential character of disc rotation. Moreover, this source is universal, as astrophysical discs actually always rotate differentially. The complication is due to the nonnormal character of flows with inhomogeneous kinematics (such as differential rotation). The nonnormality and its consequences were well understood and precisely described by the hydrodynamic community in the 90s of the last century. The imperfection of the traditional/modal analysis (spectral expansion of perturbations in time and subsequent examination of eigenfunctions) in regard to smooth (without inflection point) inhomogeneous/shear flows was revealed: operators existing in the mathematical formalism of the modal analysis of shear flows (e.g. plane Couette and Poiseuille) are nonnormal and, hence, corresponding eigenfunctions are nonorthogonal and strongly interfere (Reddy, Schmid &

⋆ E-mail: g.mamatsashvili@astro-ge.org

Henningson 1993; Trefethen et al. 1993). Consequently, a correct approach should fully analyse the interference of eigenfunctions, which is actually calculable/manageable for asymptotically large times. In fact, in the modal analysis the main focus is on the asymptotic stability of flows, while no attention is directed to any particular initial value or finite time period of the dynamics – this period of the evolution is thought to be of no significance and is left to speculation. This fact prompted the above mentioned revision of the generally accepted spectral/modal approach with the special emphasis being shifted from the analysis of long time asymptotic flow stability to the study of finite time (transient) behaviour. It was demonstrated that just because of this nonnormality of the operators, a strong linear transient growth of vortex and/or wave mode perturbations occurs in asymptotically stable (in accordance with Rayleigh's stability criterion; Rayleigh 1880) hydrodynamic shear flows (Gustavsson 1991; Butler & Farrell 1992; Reddy & Henningson 1993; Farrell & Ioannou 1993; Farrell & Ioannou 2000), that determines the fate of a flow.

Differential rotation (i.e., the disc flow nonnormality) is determinant in a number of cases. Even when other basic factors (e.g. self-gravity, stratification) are involved, it interplays with them and strongly modifies the dynamical picture. This circumstance attaches great importance to disc flow shear (nonnormality) induced phenomena. *The main goal of this paper is to study the dynamical manifestations of the nonnormality in a simple model of self-gravitating astrophysical discs.* Specifically, we consider the linear dynamics of two-dimensional perturbations in thin self-gravitating gaseous discs in the shearing sheet approximation (Goldreich & Lynden-Bell 1965). This system includes two modes of perturbations – vortex and (spiral density) wave. The distinguishing features of these modes are the following: the vortex mode is aperiodic and has nonzero potential vorticity; the SD wave mode is oscillatory and has zero potential vorticity. We use the nonmodal approach instead of modal/spectral one in describing the linear dynamics of perturbations. This approach was applied in previous well-known papers (Goldreich & Lynden-Bell 1965; Julian & Toomre 1966; Goldreich & Tremaine 1978; Toomre 1981), but they concentrate on perturbations with zero potential vorticity, i.e., on SD wave mode perturbations, whereas vortex mode ones can be important as well, for example, in the angular momentum transport. This is evidenced by the references above concerning the dynamical activity of vortical perturbations in astrophysical, though non-self-gravitating, discs. We would like to emphasize that associating turbulence and angular momentum transport in self-gravitating discs only with SD waves, one in that way does not make rigorous identification (according to the value of potential vorticity) of perturbation modes and does not investigate the relative contributions/fractions of vortical and SD wave perturbations in shear stresses. In other words, the role of vortical perturbations is left out of self-gravitating disc analysis (see also Sec. 5). Considered in the present paper linear coupling of SD wave and vortex modes (see below) makes the latter more obvious participant in the angular momentum transport process, at least as an additional generator of SD waves.

We outline some possible ways of injection of nonzero vorticity perturbations discussed in the literature. Spatial inhomogeneities of entropy (temperature) distribution, that is, baroclinic instability (Klahr & Bodenheimer 2003; Klahr 2004) and Rossby wave instability (Lovelace et al. 1999), are able to generate nonzero vorticity. Random perturbations of the vorticity field may be present in a disc that forms as a result of collapse of a turbulent protostellar cloud. Accretion of clumps of gas onto a disc and convection are other possibilities for vorticity generation (see Godon & Livio 2000 for the details about the last three mechanisms).

The first dynamical manifestation of the disc flow nonnormality is a transient character of growth of both vortex and wave mode perturbations irrespective of the value of Toomre's stability parameter Q. In dynamically important regions of wavenumber plane, *vortex mode perturbations always exhibit larger growth factors than wave mode ones.* Consequently, the underestimation of the vortex mode and its transient (swing) growth may result in an incomplete dynamical picture of discs. First of all, we would like to mention the following from our investigation fact: the transient growth of vortex mode perturbations in self-gravitating discs is much stronger than in non-self-gravitating ones. Due to this fact, the presence of self-gravity (gravitational instability) might, in principle, allow for the onset of hydrodynamic turbulence in astrophysical discs. The so-called *bypass* mechanism of the onset of hydrodynamic turbulence, which was elaborated by the hydrodynamic community in the 90s (Gebhardt & Grossmann 1994; Henningson & Reddy 1994; Baggett, Driscoll & Trefethen 1995; Grossmann 2000), may play a part in the process of triggering turbulence in self-gravitating discs as well, because linear transient amplification of perturbations due to flow nonnormality, which can supply turbulence with mean flow energy, is a basis for this concept. The details of the bypass concept as applied to astrophysical discs are given in Chagelishvili et al. 2003 and in Tevzadze et al. 2003.

The second implication of flow nonnormality – the linear coupling of vortex and wave modes, which is caused by the strong shear of disc flow – is also important for the proper comprehension of disc flow dynamics. One should note that the coupling is asymmetric: vortex mode perturbations (i.e. perturbations with nonzero potential vorticity) are able to excite SD waves (i.e. perturbations with zero potential vorticity), but not vice versa. So, this asymmetric coupling lends additional significance to the vortex mode as a participant in SD waves and shocks manifestations in astrophysical discs (Bodo et al. 2005; Bodo et al. 2007).

The paper is organized as follows: physical approximations and the mathematical formalism of the problem are introduced in Sec. 2, classification of perturbations is described in Sec. 3, the numerical analysis of the linear dynamical equations, including transient growth and coupling of vortex and wave modes, is presented in Sec. 4, discussions and summary are given in Sec. 5.

2 PHYSICAL MODEL AND EQUATIONS

Let us study the linear dynamics of vortex and wave mode perturbations in a simple analogue to a differentially rotating disc – in a thin self-gravitating gas sheet, where unperturbed velocity field is a parallel flow with a constant shear (the shearing sheet approximation). A Coriolis force

is included to take into account the effects of disc rotation. The equation of state is assumed to be polytropic. In this case, the linearized dynamical equations read as (Goldreich & Tremaine 1978):

$$\frac{\partial\sigma}{\partial t}+2Ax\frac{\partial\sigma}{\partial y}+\Sigma_0\left(\frac{\partial u}{\partial x}+\frac{\partial v}{\partial y}\right)=0, \tag{1}$$

$$\frac{\partial u}{\partial t}+2Ax\frac{\partial u}{\partial y}-2\Omega_0 v=-\frac{\partial}{\partial x}\left(c_s^2\frac{\sigma}{\Sigma_0}+\psi\right) \tag{2}$$

$$\frac{\partial v}{\partial t}+2Ax\frac{\partial v}{\partial y}+2Bu=-\frac{\partial}{\partial y}\left(c_s^2\frac{\sigma}{\Sigma_0}+\psi\right). \tag{3}$$

This set of linear perturbation equations is supplemented by Poisson's equation

$$\Delta\psi=4\pi G\sigma\delta(z). \tag{4}$$

Here u, v, σ and ψ are, respectively, the perturbed radial and azimuthal velocities, surface density and gravitational potential of the gas sheet with spatially constant unperturbed surface density Σ_0. Ω_0 is the angular velocity of the shearing sheet, c_s is the sound speed in the gas, x and y are, respectively, the radial and azimuthal coordinates of the shearing sheet, A is the Oort constant (shear parameter), which is $A/\Omega_0\simeq-0.75<0$ for quasi-Keplerian rotation considered in this paper, and $B\equiv A+\Omega_0$. As usual, we define the epicyclic frequency κ by $\kappa^2\equiv 4B\Omega_0$.

Following the standard procedure of nonmodal analysis (Goldreich & Lynden-Bell 1965; Goldreich & Tremaine 1978; Nakagawa & Sekiya 1992; Chagelishvili et al. 1997), we introduce the spatial Fourier harmonics (SFHs) of perturbations with time-dependent phases:

$$F(\mathbf{r},t)\sim F(k_x,k_y,t)\exp[\mathrm{i}k_x(t)x+\mathrm{i}k_y y], \tag{5}$$

$$k_x(t)=k_x-2Ak_y t,$$

where $F\equiv(u,v,\sigma,\psi)$. The streamwise/azimuthal wavenumber k_y remains unchanged. The streamcross/radial wavenumber $k_x(t)$ changes with time at a constant rate due to the effect of the shearing background on wave crests. One can say that in the linear approximation SFHs "drift" along the k_x-axis in $\mathbf{k}$-plane (wavenumber plane). In other words, lines of constant phase of each SFH are sheared over by the basic flow in physical plane. So, imposing initially any kind (vortex or/and wave mode) of a leading SFH ($k_x(0)/k_y<0$) on the flow, in the linear regime, it eventually becomes a trailing one ($k_x(t)/k_y>0$) as time passes. It should also be noted that SFHs represent the simplest/basic "elements" of dynamical processes at constant shear rate and greatly help to grasp the phenomena of transient growth and coupling of perturbation modes.

Substituting equation (5) into equations (1-4) and introducing $\hat\sigma\equiv i\sigma/\Sigma_0$, $\phi\equiv i\psi$, we get the system of ordinary differential equations that govern the linear dynamics of SFHs of perturbations:

$$\frac{d\hat\sigma(t)}{dt}=k_x(t)u(t)+k_y v(t). \tag{6}$$

$$\frac{du(t)}{dt}-2\Omega_0 v(t)=-k_x(t)\left[c_\mathrm{s}^2\hat\sigma(t)+\phi(t)\right], \tag{7}$$

$$\frac{dv(t)}{dt}+2Bu(t)=-k_y\left[c_\mathrm{s}^2\hat\sigma(t)+\phi(t)\right], \tag{8}$$

$$\phi(t)=-\frac{2\pi G\Sigma_0}{k(t)}\hat\sigma(t), \tag{9}$$

where $k(t)=(k_x^2(t)+k_y^2)^{1/2}$. The last equation follows from Poisson's equation and is straightforward to derive (Goldreich & Tremaine 1978; Nakagawa & Sekiya 1992).

One can easily show that this system possesses an important time invariant:

$$k_x(t)v(t)-k_y u(t)+2B\hat\sigma(t)\equiv\mathcal{I}, \tag{10}$$

which follows (for SFHs of perturbations) from the conservation of potential vorticity. This time invariant $\mathcal{I}$, in turn, indicates the existence of the vortex/aperiodic mode in the perturbation spectrum. Clarification of the role of this mode in the disc flow dynamics represents the primary purpose of our study.

In the calculations below, we use the quadratic form (spectral energy density) for a separate SFH as a measure of its intensity:

$$E(t)\equiv\frac{\Sigma_0}{2}\left(|u|^2+|v|^2\right)+\frac{\Sigma_0}{2}c_s^2|\hat\sigma|^2, \tag{11}$$

where the two terms correspond to the kinetic and potential energies of SFH, respectively. Strictly speaking, this is not an exact expression for perturbation energy, since it does not contain terms corresponding to gravitational energy. Nevertheless, we find this quadratic form convenient for a comparative analysis of transient growth of perturbation modes at different values of Toomre's parameter Q presented below.

The numerical study of SFH's dynamics is based on equations (6-11). However, for the comprehension of the dynamical processes – transient growth and coupling of vortex and SD wave modes and – it is advisable to rewrite them in the form of a single second order inhomogeneous differential equation for ϕ. Introducing dimensionless parameters and variables: $\tau\equiv t\kappa$, $K_y\equiv c_\mathrm{s}k_y/\kappa$, $K_x(\tau)\equiv c_\mathrm{s}k_x(t)/\kappa$, $K(\tau)\equiv c_\mathrm{s}k(t)/\kappa$, $\hat\Omega_0\equiv\Omega_0/\kappa\simeq 1$, $\hat A\equiv A/\kappa\simeq -0.75$, $\hat B\equiv B/\kappa\simeq 0.25$, $\hat{\mathcal{I}}\equiv\mathcal{I}/\kappa$, $Q\equiv c_\mathrm{s}\kappa/\pi G\Sigma_0$, $\hat u\equiv u/c_\mathrm{s}$, $\hat v\equiv v/c_\mathrm{s}$, $\hat\phi\equiv\phi/c_\mathrm{s}^2$, $\hat E(\tau)\equiv E(t)/\Sigma_0 c_\mathrm{s}^2$, one finally gets:

$$K_x(\tau)\hat v(\tau)-K_y\hat u(\tau)+2\hat B\hat\sigma(\tau)\equiv\hat{\mathcal{I}}, \tag{12}$$

$$\hat E(\tau)\equiv\frac{1}{2}\left(|\hat u|^2+|\hat v|^2+|\hat\sigma|^2\right), \tag{13}$$

$$\frac{d^2\hat\phi(\tau)}{d\tau^2}+\hat\omega^2(\tau)\hat\phi(\tau)=-\frac{4}{QK(\tau)}\left(\hat\Omega_0+\frac{2\hat AK_y^2}{K^2(\tau)}\right)\hat{\mathcal{I}}, \tag{14}$$

where

$$\hat\omega^2(\tau)=1+K^2(\tau)-\frac{2}{Q}K(\tau)+\frac{12\hat A^2K_y^4}{K^4(\tau)}+\frac{8\hat\Omega_0\hat AK_y^2}{K^2(\tau)}. \tag{15}$$

We retain $\hat A$ (equal to -0.75) in equations (14) and (15) to make obvious the role of the flow shear in the perturbation dynamics. The rhs of equation (14) can be viewed as a source term for SD waves (see below) and it resembles the bar term in Goldreich & Tremaine 78. All other perturbed quantities are easily expressed in terms of $\hat\phi(t)$ and its time derivative. We do not give those expressions here. Notice that due to the varying radial wavenumber $K_x(\tau)$, frequency $\hat\omega$ is also dimedependent and, as a result (we will show that below), the modes of perturbations appear to be coupled in the linear theory.

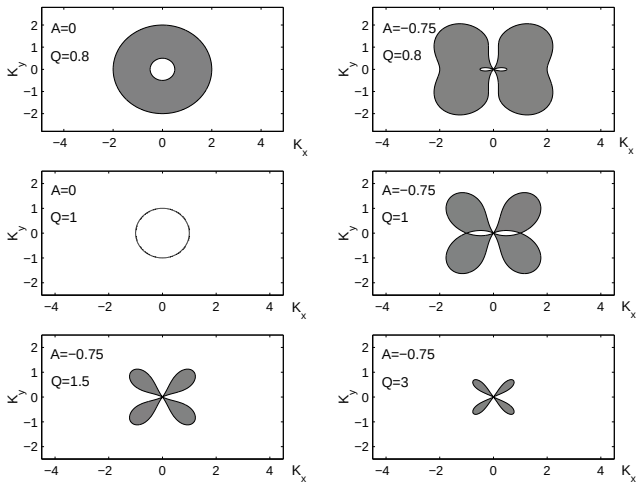

Figure 1. Unstable ($\hat{\omega}^2 < 0$) domains (grey) in **K**-plane for various values of Q. At $Q < 1$, unstable domains exist even in the shearless limit. At $Q \geq 1$, compared with $A = 0$ case, shear leads to the emergence of unstable domains. The last two panels are given only for $A \neq 0$, since there are no unstable domains in the shearless limit at $Q \geq 1$.

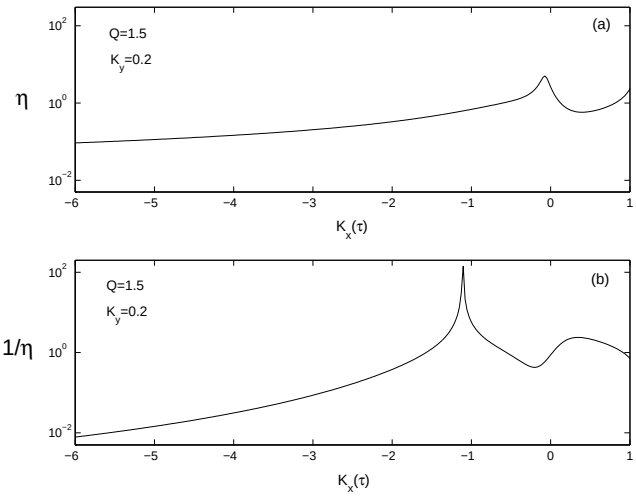

Figure 2. Panel (a) is the evolution of η in the case where a leading pure SD wave mode SFH with only one sign (positive) of frequency is inserted initially into equations (6-9). This wave mode SFH acquires curl at about the time when it starts to enter the unstable (nonadiabatic) domain in Figs. 1,4. Panel (b) shows the evolution of $1/\eta$ for an initially inserted leading pure vortex mode SFH. This vortex mode SFH acquires divergent nature at about the same time. In both figures, $Q = 1.5$ and $K_y = 0.2$.

For further reference, in Fig. 1 we show unstable ($\hat{\omega}^2 < 0$) domains in **K**-plane for various Q. At $Q < 1$, the unstable domains exist even in the shearless limit, while at $Q \geq 1$, their occurrence is brought about just by the combined action of shear and self-gravity.

3 CLASSIFICATION OF PERTURBATIONS

One can classify perturbation modes involved in equation (14) (or in equations (6-9)) from the mathematical and physical standpoints separately.

Mathematically, a general solution of equation (14) can be written as a sum of two parts: a *general* solution of the corresponding homogeneous equation (oscillatory SD wave mode) and a *particular* solution of this inhomogeneous equation. It should be emphasized that the particular solution is not uniquely determined: the sum of a particular solution of the inhomogeneous equation and any particular solution of the corresponding homogeneous equation (i.e. wave mode solution) is also a particular solution of the inhomogeneous equation, i.e., a particular solution may comprise any amount of the wave mode.

Physically, equation (14) describes two different modes/types of perturbations:
(a) SD wave mode ($\hat{\phi}^{(\mathrm{w})}$), that is determined by general solution of the corresponding homogeneous equation and has zero potential vorticity ($\hat{\mathcal{I}} = 0$);
(b) Vortex mode ($\hat{\phi}^{(\mathrm{v})}$), originating from the equation inhomogeneity (the rhs of equation (14)), is associated with the nonoscillatory part of a particular solution of the inhomogeneous equation. In the shearless limit, the vortex mode is independent of time and has zero velocity divergence, but nonzero potential vorticity. However, in the presence of a shear it acquires divergence as well (this question is addressed in detail below). From the above argument, it follows that the correspondence between the aperiodic vortex mode and the particular solution of the inhomogeneous equation is quite unambiguous – the vortex mode is associated only with that part of a particular solution not containing any oscillations. The amplitude of the vortex mode is proportional to $\hat{\mathcal{I}}$ and goes to zero when $\hat{\mathcal{I}} = 0$.

In the following, we will keep to the physical standpoint of separation of perturbation modes. Thus, any solution of equations (6-9) can be expressed as a superposition of oscillatory/SD wave and aperiodic/vortex modes:

$$\hat{u} = \hat{u}^{(\mathrm{w})} + \hat{u}^{(\mathrm{v})},\ \hat{v} = \hat{v}^{(\mathrm{w})} + \hat{v}^{(\mathrm{v})},$$
$$\hat{\sigma} = \hat{\sigma}^{(\mathrm{w})} + \hat{\sigma}^{(\mathrm{v})},\ \hat{\phi} = \hat{\phi}^{(\mathrm{w})} + \hat{\phi}^{(\mathrm{v})},$$

where $\hat{u}^{(\mathrm{w})}$, $\hat{v}^{(\mathrm{w})}$, $\hat{\sigma}^{(\mathrm{w})}$ and $\hat{u}^{(\mathrm{v})}$, $\hat{v}^{(\mathrm{v})}$, $\hat{\sigma}^{(\mathrm{v})}$ are found from $\hat{\phi}^{(\mathrm{w})}$ and $\hat{\phi}^{(\mathrm{v})}$ respectively.

In fact, the (modified) initial value problem is solved by equations (6-9) (or, equivalently, by equations (12-14)). The character of the dynamics depends on the mode of perturbation inserted initially into equations (6-9): pure SD wave mode (without admixes of aperiodic vortices) or pure aperiodic vortex mode (without admixes of SD waves).

Classification of perturbation modes that is widespread divides them into vortical and divergent types. Such a classification coincides with the described above physical classification in the case of nonvortical (rigid) mean rotation, when the wave mode has zero potential vorticity, but nonzero divergence and the vortex mode has zero divergence, but nonzero potential vorticity. In the considered quasi-Keplerian (i.e. strongly sheared) flow, the situation is fundamentally different: the vortex mode may acquire divergent nature and initially predominantly divergent wave mode may acquire curl in the course of evolution.

In Fig. 2 we present the time-development of the parameter:

$$\eta = \left| \frac{K_x(\tau)\hat{v}(\tau) - K_y\hat{u}(\tau)}{K_x(\tau)\hat{u}(\tau) + K_y\hat{v}(\tau)} \right|,$$

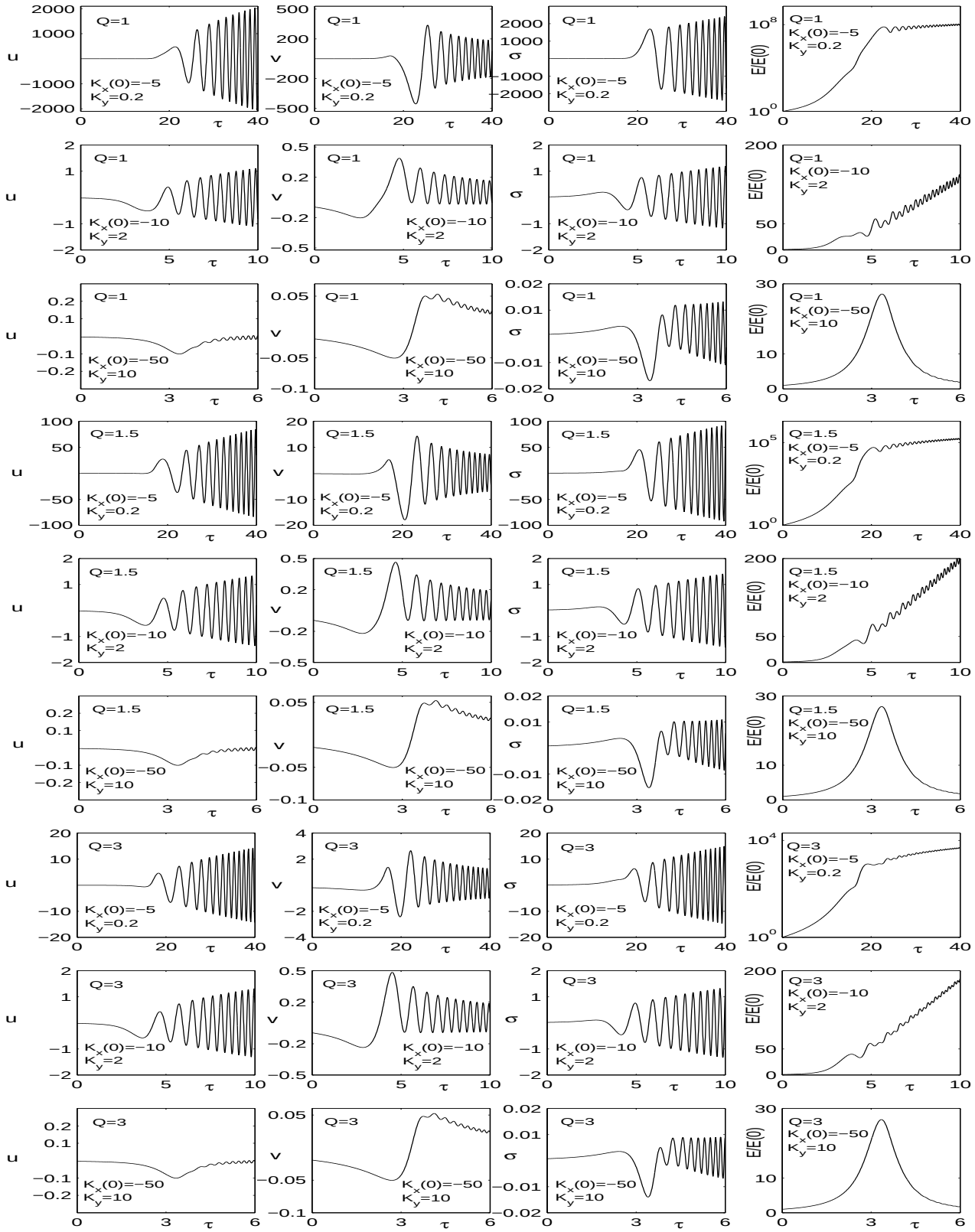

Figure 3. Evolution of perturbed quantities pertaining to an initially imposed leading pure vortex mode SFH at different Q, $K_x(0)$ and K_y (corresponding values are shown in each panel). Before reaching the first unstable domain, the vortex mode SFH gains energy from the mean flow and amplifies, but retains its aperiodic nature. In the unstable domains, oscillations (SD waves) begin to appear. The energy increases monotonically and then, after going through the unstable domains, asymptotically linearly corresponding to the generated SD waves (for $K_yQ < 2$, the energy curves are in logarithmic scale, so the flat part is actually linear growth). The contribution of the vortex mode energy to the total perturbation energy is negligible at this asymptotic stage. The vortex mode simply dies down giving way to trailing SD waves. The wave generation is very effective for $K_yQ < 2$, moderate for $K_yQ \sim 2$ and vanishing for $K_yQ \gg 2$.

which represents the ratio of the z-component of curl to divergence, and its inverse value $1/\eta$ for initially imposed SD wave and vortex mode SFHs respectively. In the case where initially a predominantly divergent leading pure SD wave mode SFH with positive frequency is inserted into equations (6-9) (the procedure for selecting this type of initial condition is described in detail in Nakagawa & Sekiya 1992), it acquires curl at about the time of entering the unstable (nonadiabatic) domain in Figs. 1,4, as seen in Fig. 2(a). Fig. 2(b) shows that an initially inserted leading pure vortex mode SFH acquires divergent nature at about the same time.

Thus, divergent (or vortical) perturbations in the quasi-Keplerian flow (or, in a shear flow in general) represent some mix of vortex and wave modes and classification of perturbations as vortical and divergent may be misleading. So, we prefer the classification of perturbations into wave and vortex modes and investigate dynamical processes in terms of dynamics of these two modes.

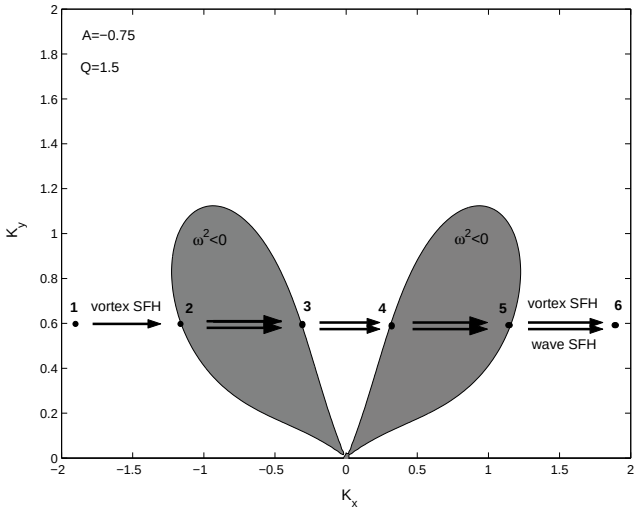

Figure 4. Sketch of SFH's evolution in **K**-plane. A leading vortex mode SFH, located initially at point 1, drifts with time along the K_x-axis in the direction denoted by the arrows $1 \to 2 \to 3 \to 4 \to 5 \to 6$. After crossing point 2, a SD wave mode SFH appears. The first stage of the wave excitation takes place from point 2 to point 3, the second one – from point 4 to point 5.

4 TRANSIENT GROWTH AND COUPLING OF VORTEX AND SD WAVE MODE SFHs – NUMERICAL ANALYSIS

We begin the numerical integration of equations (6-9), choosing as an initial condition leading ($K_x(0)/K_y < 0$) pure vortex mode SFH without any admixes of SD wave mode SFHs. Such a selection of the vortex mode is possible only far from the unstable domains, where $|K_x(\tau)/K_y| \gg 1$ and the adiabatic condition $|d\hat{\omega}(\tau)/d\tau| \ll \hat{\omega}^2(\tau)$ is met. The procedure for selecting is described in detail in the Appendix of Bodo et al. 2005. In Fig. 3, we present the subsequent evolution of $\hat{u}$, $\hat{v}$, $\hat{\sigma}$ and $\hat{E}/\hat{E}(0)$ for this kind of initial condition at different values of Q and K_y (in these and other figures below, hats are omitted). The sketch of the SFH's evolution/drift in wavenumber plane is given in Fig. 4. We single out a leading SFH, for which $K_y < 2Q^{-1}$ and that is located initially at point 1 far from the unstable domains and coincides here, as mentioned above, with a pure vortex mode SFH (henceforth, we take the azimuthal wavenumber K_y to be positive without loss of generality). As seen in this figure, this SFH drifts along the K_x-axis in the direction denoted by the arrows ($1 \to 2 \to 3 \to 4 \to 5 \to 6$). The drift velocity ($= 2K_y|\hat{A}|$) depends linearly on K_y. Initially, being in the adiabatic region, the SFH gains energy from the mean flow due to the nonnormality and amplifies algebraically, but retains its aperiodic nature. Then, the dynamics becomes nonadiabatic – the SFH reaches the unstable domain where $\hat{\omega}^2(\tau) < 0$ (point 2). From this point, a temporal exponential growth and simultaneous excitation of the corresponding SFH of SD wave mode take place – at this stage of the evolution, the linear coupling of vortex and wave mode SFHs is at work (this phenomenon was found and thoroughly described for the simplest shear flow in Chagelishvili et al. 1997 and for non-self-gravitating Keplerian discs in Bodo et al. 2005). Then, the vortex and the generated SD wave mode SFHs reach the intermediate stable region (point 3) where $\hat{\omega}^2(\tau) > 0$, pass it and get again into the domain where $\hat{\omega}^2(\tau) < 0$ (point 4). Further exponential growth of both vortex and SD wave mode SFHs and, in addition, excitation of another SD wave mode SFH by the vortex mode one occur until they cross this second unstable domain (point 5). After that, the linear dynamics of the vortex and SD wave mode SFHs become decoupled and adiabatic: the energy of the vortex mode SFH dies down and the energy of the wave mode SFHs increases. No further SD wave excitation is observed beyond point 5.

Here we have described the SD wave generation for $K_y < 2Q^{-1}$, although it similarly occurs for $K_y \sim 2Q^{-1}$ (see Fig. 3), except that the transient amplification of an initially imposed vortex mode SFH is mainly due to the nonnormality, since the unstable domains do not extend to such K_y. As a consequence, the amplification amount and the amplitudes of generated SD wave mode SFHs are several orders of magnitude lower than those for $K_y < 2Q^{-1}$.

Thus, the linear dynamics of a vortex mode SFH is followed by the generation of the corresponding SD wave mode SFHs. This generated SFHs eventually acquire a trailing orientation, since $K_x(\tau)/K_y > 0$ after leaving the nonadiabatic region (that stretches roughly from point 2 to point 5 in Fig. 4). In the nonadiabatic region, the characteristic timescales of the vortex and SD wave mode SFHs are comparable and the perturbation modes cannot be separated/distinguished. But with moving away from the nonadiabatic region, modes get cleanly separated: the timescale of the SD wave mode SFHs becomes much shorter than that of the vortex mode SFH (the frequency of waves increases with time). One can formally divide the energy evolution into two stages: the first stage represents the transient amplification (both due to the nonnormality and to the unstable domains) of the originally imposed pure vortex mode SFH and excitation (and also subsequent exponential amplification) of the corresponding SFHs of SD wave mode, and the second one represents the algebraic growth of the generated SD wave mode SFHs. The latter exhibit linear amplification at asymptotically large times. In the absence of the wave excitation (e.g. for $K_y \gg 2Q^{-1}$), this second stage

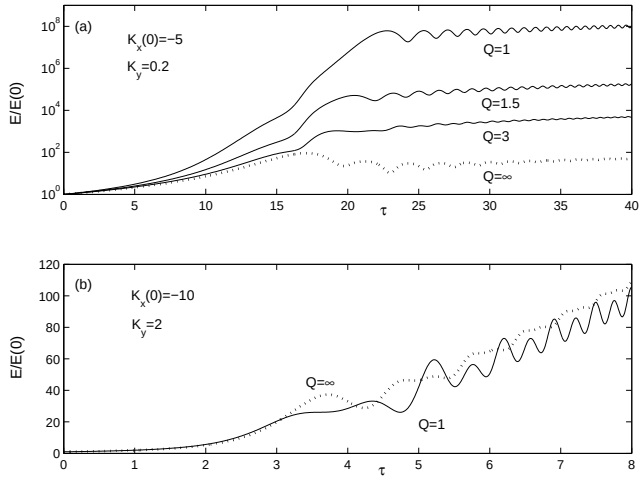

Figure 5. Influence of self-gravity on the transient (swing) amplification of a vortex mode SFH (dotted lines correspond to the non-self-gravitating case). This influence is, as expected, largest for $K_yQ < 2$ (panel (a), all four curves are characterized by the same $K_x(0) = -5,\ K_y = 0.2$ and identical initial values of perturbed quantities) and negligible for $K_yQ \sim 2$ (panel (b), $K_x(0) = -10,\ K_y = 2$).

describes decreasing energy of a vortex mode SFH. Thus, newly created trailing SD wave mode SFHs in the linear regime extract energy from the mean quasi-Keplerian flow in contrast to a trailing vortex mode SFH that after leaving the nonadiabatic region, gradually returns all its energy to the mean flow. One can say that vortex mode perturbations act as a mediator between the mean flow and waves. The energy needed for the wave excitation is extracted from the shear and self-gravity with the help of the vortex mode.

The following two subsections are devoted to the behaviour of vortex mode perturbations for various values of Toomre's parameter Q.

4.1 Effect of self-gravity on the transient growth of vortex mode perturbations

In Fig. 5, we compare the time-development of $\hat{E}/\hat{E}(0)$ for initially imposed vortex mode SFHs in the presence and absence of self-gravity for different values of Q and K_y. It is clear that the growth of vortex mode SFHs continues longer time and may be several orders of magnitude stronger than in the non-self-gravitating case ($Q \to \infty$, dotted lines in the panels). In this case, the growth of vortex mode SFHs occurs just at the leading stage ($K_x(\tau)/K_y < 0$), on becoming trailing ($K_x(\tau)/K_y > 0$) SFHs give back energy to the mean flow and weaken (Chagelishvili et al. 2003). In the self-gravitating case instead, the amplification of SFHs continues into the trailing stage as well due to the existence of the unstable domain at $K_x(\tau)/K_y > 0$ (see Figs. 1,4). From Fig. 5, one can see that at $Q = 1$ and $K_y = 0.2$, a vortex mode SFH grows about 10^6 times stronger than in the non-self-gravitating case; at $Q = 1.5$ and $K_y = 0.2$ – about 10^4 times stronger; at $Q = 3$ and $K_y = 0.2$ – about 10^2 times stronger; at $Q = 1$ and $K_y = 2$, i.e., at $K_yQ \sim 2$, the growth is the same as in the non-self-gravitating case. In any case, one can conclude that self-gravity provides a substantial enhancement of the transient growth of vortex mode perturbations, thereby making them active participants in dynamical processes. This, in turn, shows that the bypass mechanism may play a part in the onset of turbulence in self-gravitating discs.

In order to better understand the role of the vortex mode, it is interesting to carry out a comparative analysis of the transient (swing) amplification of the vortex and SD wave modes. First we define a density growth factor f for SFH initially located at point 1, as a ratio of the absolute values of $\hat{\sigma}(\tau)$ after (at point 5) and before (at point 2) crossing the unstable domains in Fig. 4, $f \equiv |\hat{\sigma}(\tau'')|/|\hat{\sigma}(\tau')|$, where τ'' and τ' are the moments corresponding to points 5 and 2 respectively. A similar growth factor for coherent wavelet solutions was used by Kim & Ostriker (2001), but they took its logarithm. In Fig. 6(a), we present this parameter computed separately for the initially imposed vortex and SD wave mode SFHs as a function of the dimensionless azimuthal wavenumber K_y at $Q = 1.5$. The initially imposed SD wave mode SFH has a certain (positive) sign of frequency. As seen in this panel, in the dynamically important regions (i.e., for such values of K_y, at which both modes experience maximum transient growth), the growth factor for the vortex mode SFH is almost two times larger than that for the SD wave mode one. An analogous comparison is made in Fig. 6(b). Here we display the ratio of the maximum value achieved by the energy $\hat{E}(\tau)$ during transient amplification in the unstable domains to its initial value on entering these domains (i.e., at point 2) computed separately for the imposed at point 2 vortex and SD wave mode SFHs as a function of K_y, similar to what is done in Fig. 6(a). But now, as distinct from the first case, for the wave mode SFH we choose initial conditions at point 2 in such a way as to obtain the largest possible amplification of the wave energy in the transient growth (swing) phase for its fixed initial value, i.e., we take transiently most unstable wave mode SFH. The situation is similar to the above one: the energy amplification factor for the vortex mode SFH is more than two times greater than the largest possible energy amplification factor for the SD wave mode SFH. In Fig. 6(c), we present the parallel evolution of the energies of the initially (at point 2) imposed vortex and maximally amplified wave mode SFHs for $K_y = 0.3$, at which the energy growth factors of both modes during swing phase are the largest (see Fig. 6(b)). Both SFHs start with the same energy. This panel shows that the energy corresponding to the initially imposed vortex mode SFH remains about two times larger than that corresponding to the SD wave mode SFH at all times.

From Fig. 6, it is evident that the vortex mode prevails over the SD wave mode in two respects: in the transient amplification and wave generation (by the wave generation for the initially imposed SD wave mode SFH we mean wave amplification due to the over-reflection mechanism; see Nakagawa & Sekiya 1992 for details). The latter follows from the asymptotic stage at large times, when both energy curves become linear (see Figs. 3,6(c)) with inclinations proportional to the square of the amplitudes of generated SD wave mode SFHs after crossing the unstable domains. We see that the energy of SD wave mode SFHs generated by the initially imposed vortex mode one at this asymptotic stage is about

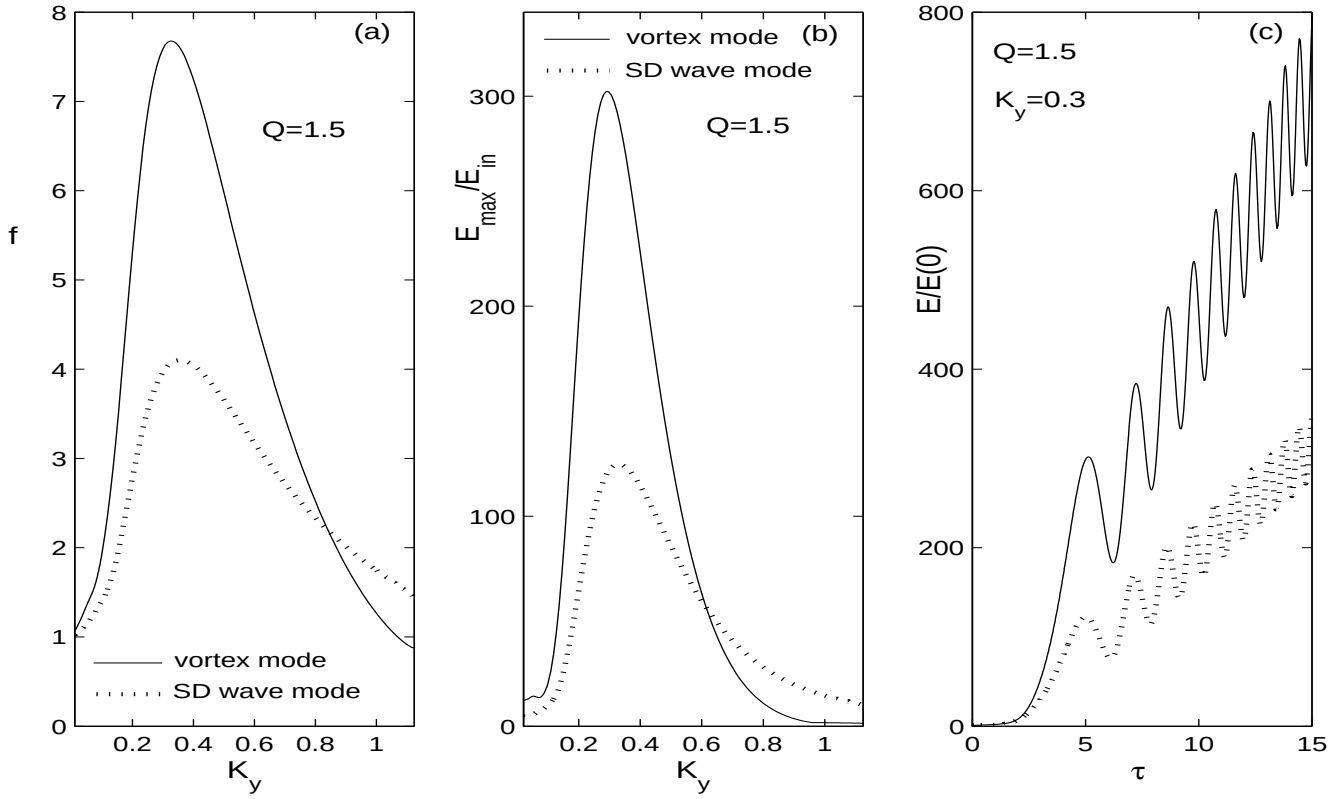

Figure 6. Growth factors of density (panel (a)) and energy (panel (b)) vs K_y. Also shown is the evolution of $\hat{E}/\hat{E}(0)$ for two cases (panel (c)). Solid curves in the panels correspond to the initially imposed vortex mode SFH, dotted curves – to the initially imposed SD wave mode SFH. In all three panels, $Q = 1.5$. In panel (c), $K_y = 0.3$. $\tau = 0$ corresponds to point 2 in Fig. 4.

two times larger than that of the generated by the initially imposed SD wave mode SFH.

4.2 Ways of SD wave generation

There are two ways of SD wave generation in the considered here disc flow. The first is a direct and well-known over-reflection mechanism: inserting a leading SD wave mode SFH in equations (6-9), one can get the energy dynamics represented by the dotted curve in Fig. 6c. The curve describes the energy growth in the unstable domains that is followed by a linear growth of the total energy of the resulting over-reflected and (over)-transmitted trailing SD wave mode SFHs at large times.

Another way of the generation of trailing SD wave mode SFHs is by means of vortex mode SFHs: leading pure vortex mode SFHs can effectively excite trailing SD wave mode ones due to the mode coupling phenomenon. Figure 6 shows that this second way of SD wave generation is about two times more effective than the first one.

We go on to calculate the amplitudes of SD waves generated due to mode coupling (more precisely, the amplitudes for the gravitational potential perturbations. The amplitudes for other quantities can afterwards be found easily). Insert an adiabatic leading vortex mode SFH into equation (14). Then after passing the nonadiabatic region (in the other adiabatic region at $\tau \to \infty$) this solution goes over to the superposition of a trailing SFH of the vortex mode and generated SD wave mode SFHs:

$$\hat{\phi}(\tau) = \hat{\phi}^{\rm v}(\tau) + \hat{\phi}^{\rm w}(\tau) = -\frac{4}{QK(\tau)\hat{\omega}^2(\tau)}\left(\hat{\Omega}_0 + \frac{2\hat{A}K_y^2}{K^2(\tau)}\right)\hat{\mathcal{I}} + \\ + \frac{a}{Q\sqrt{\hat{\omega}(\tau)}}e^{-i\int^\tau \hat{\omega}(\tau')d\tau'} + \frac{a^*}{Q\sqrt{\hat{\omega}(\tau)}}e^{i\int^\tau \hat{\omega}(\tau')d\tau'},$$

where a and a^* are the amplitudes of generated SD wave mode SFHs. The latter come in complex conjugate pairs with different signs of frequencies and, hence, propagating in the opposite directions. In Fig. 7, we plot the numerically obtained $|a|$ as a function of K_y at $Q = 1.5$ and in Fig. 8 the same for different values of Q. In both figures $\hat{\mathcal{I}}$ is set to unity. The procedure for the calculations is analogous to that employed by Nakagawa & Sekiya (1992) to study the over-reflection of SD waves.

Let us analyse the curves in Figs. 7,8. The maximum value of $|a|$ is achieved for $K_y \sim O(0.1)$, as at such K_y a SFH drifts slowly in **K**-plane, consequently, slowly crosses the unstable domains and has more time for transient growth. The cavities in these figures are due to the crossing of two wave excitation domains by the SFH (see Fig. 4) and, therefore, due to the existence of two, more or less independent, stages of the wave excitation/generation: the resulting (after leaving both unstable domains) wave mode SFH is a superposition of SFHs generated at these stages. At $Q = 1.5$, this interference is destructive close to $K_y = 1$ and results in the cavity (Fig. 7). As one can see from Fig. 8, the cavity point occurs at different K_y for different Q. At small values of Q, the number of cavity points increases (see curve for $Q = 1$ in Fig. 8), as destructive interference happens at dif-

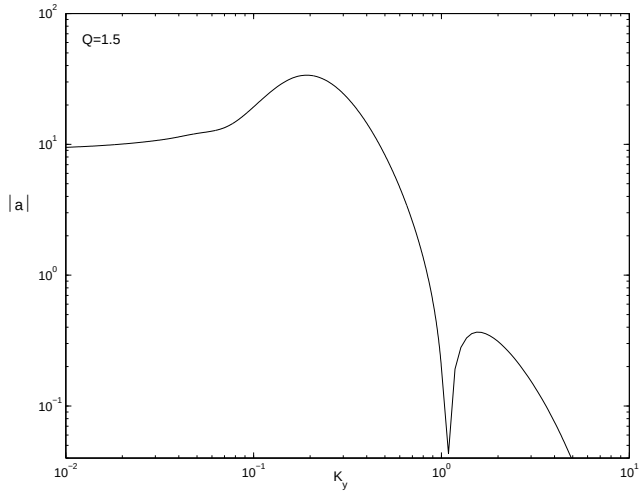

Figure 7. The amplitude $|a|$ of trailing SD wave mode SFH generated by a leading vortex mode SFH vs K_y at $Q = 1.5$.

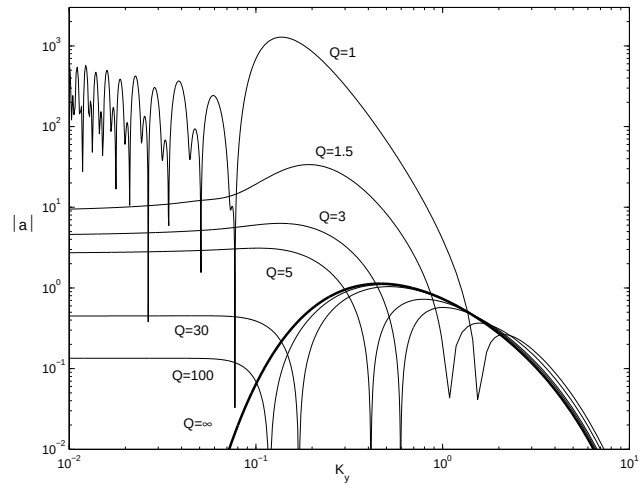

Figure 8. Same as in Fig. 7, but for different values of Q, including the non-self-gravitating case ($Q \to \infty$).

ferent K_y. In the non-self-gravitating case ($Q \to \infty$), there is no cavity point, as in this case there is just one stage of the wave excitation and, therefore, the interference phenomenon is absent.

5 SUMMARY AND DISCUSSIONS

Studying flow nonnormality induced transient phenomena in thin self-gravitating astrophysical discs, we have concentrated on the dynamics of vortex mode perturbations. The linear dynamics of perturbations has been investigated by means of so-called nonmodal approach, which consists in tracing the dynamics of SFHs (see equation (5)). SFHs represent the simplest/basic "elements" of the dynamical processes at constant shear rate and greatly help to grasp transient growth and coupling of perturbation modes. It has been shown that self-gravity considerably alters the dynamics of vortex mode SFHs – their transient growth may be several orders of magnitude stronger than in the non-self-gravitating case and 2-3 times larger than the transient growth of the wave mode (see Figs. 5,6).

The evolution of vortical and wave type perturbations has recently been studied by Wada, Meurer & Norman (2002) in high-resolution numerical simulations of two-dimensional hydrodynamic turbulence in certain galactic disc flows. These simulations clearly demonstrate that vortical/solenoidal perturbations are equally important together with spiral density wave/compressible perturbations in determining the properties (spectra) of the resulting gravitoturbulent state. They also suggest, based on their simulation results, that self-sustained turbulence can also occur in the case of self-gravitating Keplerian rotation. Their work supports the conclusion that the described here gravity-enhanced transient growth of a vortex mode perturbation is a key factor in the simulated self-sustained turbulence and, hence, the vortex mode perturbation itself – a key participant. Consequently, self-gravity, or gravitational instability, might allow for the onset of two-dimensional hydrodynamic turbulence in astrophysical disc flows and the bypass mechanism of the onset of turbulence (elaborated by the hydrodynamic community in the 90s of the last century), may play a part in this process.

Another relevant to the present paper work is that of Gammie (2001). In this paper, turbulence and angular momentum transport in self-gravitating discs are studied numerically in the shearing sheet approximation. One has to note that the initial white noise distribution adopted by Gammie (2001), in fact, includes also vortex mode perturbations, as the potential vorticity of the initially imposed white noise is nonzero, i.e., the initial perturbation is a mixture of vortex and wave modes. However, as mentioned in the Introduction, the identification/separation of the modes and the separate study of their properties have been left out of analysis. In the case of such a mixture, vortex mode perturbations grow transiently and at the same time generate zero vorticity perturbations (i.e., SD waves) via the described here linear mechanism. The resulting turbulence can be more "violent" than the zero vorticity one, i.e., turbulence in which the basic elements are SD waves, and therefore the angular momentum transport can be more intense because of the larger transient growth factors of vortex mode perturbations. There should also be differences in the statistical properties (energy spectra) of these two kinds of turbulence. (This question is addressed, in part, in Wada, Meurer & Norman 2002. However, they make somewhat different from ours classification of perturbation modes). Gammie's analysis actually concentrates only on the question of locality of angular momentum transport in a gravitoturbulent state and not on the investigation of the relative contributions/fractions of vortex and SD wave mode perturbations in shear stresses governing angular momentum transport in discs.

The described linear coupling of vortex and wave modes, which is caused by the differential character of the disc flow, is asymmetric: vortex mode perturbations are able to generate wave mode ones, but not vice versa. The considered system conserves potential vorticity and it is obvious that vortex mode perturbations, having nonzero vorticity, are able to excite SD wave mode perturbations having zero potential vorticity. This asymmetric coupling lends ad-

ditional significance to the vortex mode as a participant in SD waves and shocks manifestations in astrophysical discs.

ACKNOWLEDGMENTS

This work is supported by the International Science and Technology Center (ISTC) grant G-1217. We would like to thank the anonymous referee for helpful comments.

REFERENCES

Afshordi N., Mukhopadhyay B., Narayan R., 2005, ApJ, 629, 373
Baggett J. S., Driscoll T. A., Trefethen L. N., 1995, Phys. Fluids, 7, 833
Barge P., Sommeria J., 1995, A&A, 295, L1
Bodo G., Chagelishvili G., Murante G., Tevzadze A., Rossi P., Ferrari A., 2005, A&A, 437, 9
Bodo G., Tevzadze A., Chagelishvili G., Mignone A., Rossi P., Ferrari A., 2007, submitted to A&A
Bracco A., Chavanis P. H., Provenzale A., Spiegel E., 1999, Phys. Fluids, 11, 2280
Butler K. M., Farrell B. F., 1992, Phys. Fluids A, 4, 1637
Chagelishvili G. D., Tevzadze A. G., Bodo G., Moiseev S. S., 1997, Phys. Rev. Lett., 79, 3178
Chagelishvili G., Zahn J-P., Tevzadze A., Lominadze J., 2003, A&A, 402, 401
Davis S. S., Sheehan D. P., Cuzzi J. N., 2000, ApJ, 545, 494
Davis S. S., 2002, ApJ, 576, 450
Farrell B. F., Ioannou P. J., 1993, Phys. Fluids A, 5, 1390
Farrell B. F., Ioannou P. J., 2000, Phys. Fluids, 12, 3021
Fridman A. M., Khoruzhii O. V., 1999, in Sellwood J. A. and Goodman J., eds, ASP Conf. Ser. Vol. 160, Astrophysical Discs. Astron. Soc. Pac., San Francisco, p. 341
Gammie C., 2001, ApJ, 553, 174
Gebhardt T., Grossmann S., 1994, Phys. Rev. E, 50, 3705
Godon P., Livio M., 1999, ApJ, 523, 350
Godon P., Livio M., 2000, ApJ, 537, 396
Goldreich P., Lynden-Bell D., 1965, MNRAS, 130, 125
Goldreich P., Tremaine S., 1978, ApJ, 222, 850
Grossmann S., 2000, Rev. Mod. Phys., 72, 603
Gustavsson L. H., 1991, J. Fluid Mech., 224, 241
Henningson D. S., Reddy S. C., 1994, Phys. Fluids, 6, 1396
Ioannou P. J., Kakouris A., 2001, ApJ, 550, 931
Johnson B. M., Gammie C. F., 2005, ApJ, 635, 149
Julian W. H., Toomre A., 1966, ApJ, 146, 810
Kim W., Ostriker E., 2001, ApJ, 559, 70
Klahr H. H., Bodenheimer P., 2003, ApJ, 582, 869
Klahr H. H., 2004, ApJ, 606, 1070
Klahr H. H., Bodenheimer P., 2006, ApJ, 639, 432
Lodato G., Rice W. K. M., 2004, MNRAS, 351, 630
Lodato G., Rice W. K. M., 2005, MNRAS, 358, 1489
Lominadze J. G., Chagelishvili G. D., Chanishvili R. G., 1988, SvA. Lett., 14, 364
Lovelace R. V. E., Li H., Colgate S. A., Nelson A. F., 1999, ApJ, 513, 805
Mejia A. C., Durisen R. H., Pickett M. K., Cai K., 2005, ApJ, 619, 1098
Nakagawa Y., Sekiya M., 1992, MNRAS, 256, 685
Pringle J. E., 1981, ARA&A, 19, 137
Rayleigh, Lord, 1880, Scientific Papers, Vol. 1, Cambridge Univ. Press, Cambridge, p. 474
Reddy S. C., Henningson D. S., 1993, J. Fluid Mech., 252, 209
Reddy S. C., Schmid P. J., Henningson D. S., 1993, SIAM J. Appl. Math., 53, 15
Shakura N. I., Sunyaev R. A., 1973, A&A, 24, 337
Tagger M., 2001, A&A, 380, 750
Tevzadze A., Chagelishvili G., Zahn J.-P., Chanishvili R., Lominadze J., 2003, A&A, 407, 779
Toomre A., 1981, in Fall S. M. and Lynden-Bell D., eds, The Structure and Evolution of Normal Galaxies. Cambridge Univ. Press, Cambridge, p. 111
Trefethen L. N., Trefethen A. E., Reddy S. C., Driscoll T. A., 1993, Sci., 261, 578
Umurhan O. M., Regev O., 2004, A&A, 427, 855
Wada K., Meurer G., Norman C., 2002, ApJ, 577, 197
Yecko P. A., 2004, A&A, 425, 385